Bozok Journal of Science

Volume 3, No 1, Page 34-41 (2025)

Research Article DOI:10.70500/bjs.1681654

Dynamic Behavior of the Spin-1/2 Ising Model in an Oscillating External Magnetic Field

Ümüt Temizer [1*]

[1]Yozgat Bozok University, Faculty of Science and Letters, Department of Physics, 66100, Yozgat, Türkiye

[*]Correspondence: umut.temizer@bozok.edu.tr

Received: 22/04/2025	Accepted: 20/05/2025	Final Version: 27/05/2025

Abstract

The dynamic phase transition (DPT) temperatures and the dynamic phase diagrams are obtained for spin-1/2 Ising system under the presence of a time-dependent oscillating external magnetic field using the method that was purposed by Meijer and Edwards [ANNALS of PHYSICS, 54, 240 (1969)] within the framework of the Bethe or constant coupling theory. The time variation of magnetization is investigated to find the phases in the system. Thermal behavior of the average magnetization is studied to characterize the nature (continuous and discontinuous) of transitions and to obtain the dynamic phase transition temperatures. The DPT temperatures are found always a second-order; hence there can be no tricritical point separating lines of first- and second-order dynamic phase transitions. This result agrees with the dynamic Monte-Carlo (MC) simulations of a two-dimensional kinetic spin-1/2 Ising model in an oscillating external magnetic field.

Keywords: Bethe approximation; Dynamic phase transitions; Dynamic phase diagrams

1. INTRODUCTION

The equilibrium behavior of cooperative physical systems is now well understood within the framework of equilibrium statistical physics. However, their dynamic properties remain relatively unexplored, both theoretically and experimentally, due to their inherent complexity. Among the intriguing challenges in dynamic systems are dynamic phase transitions (DPTs) or nonequilibrium phase transitions, for which the underlying mechanisms have not yet been rigorously investigated and the foundational phenomenology remains underdeveloped. Therefore, continued research into these time-dependent phenomena—particularly in determining DPT points and constructing comprehensive phase diagrams—is expected to be highly rewarding. In recent years, DPTs in nonequilibrium systems under oscillating external magnetic fields have gained considerable theoretical attention (Fujiwara et.al., 2007). Experimental evidence for such transitions has been observed in a variety of systems, including highly anisotropic (Ising-like) and ultrathin Co/Cu(001) ferromagnetic films (Jiang et.al., 1995), amorphous YBaCuO films (Samoilenko et.al., 2003), ferroic systems with pinned domain walls (including ferromagnets, ferroelectrics, and ferroelastics) (Kleemann et.al., 2005), polyethylene naphthalate (PEN) nanocomposites (Kanuga and Çakmak, 2007) and cuprates (Gedik et. al., 2007).

In this study, the dynamic phase transition (DPT) is investigated within the kinetic spin-1/2 Ising model subjected to a time-dependent oscillating external magnetic field. The dynamic phase diagrams are constructed using the dynamic approach developed by Meijer and Edwards (Meijer and Edwards, 1969) within the framework of Bethe or constant coupling theory. By solving the dynamic equations, we identified the various phases present in the system. The thermal behavior of the dynamic magnetization is analyzed to determine the nature of the transitions—whether continuous or discontinuous—and to locate the dynamic phase transition temperatures. The resulting phase diagram is plotted in the plane defined by the magnetic field amplitude (H_0) and temperature (T).

It is worth noting that one of the earliest investigations into the dynamic phase transition (DPT) in the kinetic spin-1/2 Ising model under a time-dependent (sinusoidal) magnetic field was carried out by Tome and Oliveira (Tome and Oliveira, 1998). They employed Glauber-type stochastic dynamics (Glauber, 1963) to derive the mean-field dynamic equation. Their findings revealed that at high values of reduced temperature (T) and reduced magnetic field (h), the system exhibits a paramagnetic (P) phase, while at lower values of T and

[1] https://orcid.org/0009-0003-1637-2642

h, it transitions to a ferromagnetic (F) phase. The boundary separating these phases corresponds to a second-order phase transition line. Additionally, at low temperatures, they identified a region where the P and F phases coexist—termed the coexistence region (F+P)—which is bounded by a first-order phase transition line. This led to the identification of a tricritical point (TCP), where the first- and second-order transition lines converge, marking a shift in the nature of the phase transition. Later mean-field studies (Acharyya and Chakrabarti, 1995) also reported the presence of a TCP. However, Zimmer (Zimmer, 1993), through both analytical and numerical dynamic mean-field analyses, argued that previous interpretations of a TCP were likely influenced by critical slowing-down effects near the DPT, rather than indicating a true tricritical behavior. Similar conclusions were drawn by Chakrabarti and Acharyya (Chakrabarti and Acharyya , 1999), and Acharyya (Acharyya, 1999), based on dynamic Monte Carlo simulations, suggesting that the kinetic spin-1/2 Ising model undergoes a first-order phase transition and thus possesses a TCP where the transition changes from second to first order. In contrast, Korniss et al. (Korniss et al, 2002) applied classical nucleation theory to the decay of metastable phases, alongside extensive large-scale dynamic Monte Carlo simulations of a two-dimensional kinetic spin-1/2 Ising ferromagnet under an oscillating magnetic field. Their results provided strong evidence against the existence of a first-order transition at any frequency, and consequently, against the existence of a tricritical point in this context. They emphasized that although behaviors resembling a first-order transition had been correctly observed in earlier studies these were actually due to the stochastic nature of single-droplet metastable decay processes. This regime, characterized by stochastic resonance, disappears in the thermodynamic limit for systems with fixed field amplitude.

Recently, many theoretical and numerical studies have been performed in order to understand the origin of DPT. To investigate theoretically the DPT, some approximation methods such as the dynamic MC simulations (Li and Wang, 2024), (Jang et. al., 2024) dynamic mean-field theory based on the Glauber-type stochastic dynamics (Temizer, Demir, 2018) (Temizer, 2014) and dynamic effective field theory (Kantar, 2017) (Jiang, 2023) have been widely employed. In these studies, besides the DPT, the dynamic compensation temperature, dynamic phase diagrams and dynamic hysteresis behavior have been investigated, in detail.

The purpose of the present paper is, therefore, to check the validity of the method in which compare its results with the dynamic MC simulations. If its results are in good agreement with the dynamic MC simulations, we conclude or suggest that one can use this method for studying the DPT and presenting the dynamic phase diagrams in different systems instead of using the time consuming process searching dynamic critical behavior of systems while using the dynamic MC simulations.

The outline of the remaining part of this paper is organized as follows. In Section II, the model and its formulations, namely the derivation of the set of dynamic equations, are given, briefly. In Section III, the numerical results and discussion for the magnetization, average magnetization, the average nearest-neighbor-correlation, the DPT points and phase diagrams are studied in detail.

2. THE MODEL AND DERIVATION DYNAMIC EQUATIONS

The spin-1/2 model in the presence of a time-dependent oscillating external magnetic field is described by the following Hamiltonian

$$\mathcal{H} = -\frac{J}{2}\sum_{<ij>}\sigma_i\sigma_j - H\sum_{i=1}^{N}\sigma_i \tag{1}$$

where the σ_i located at the site *i* on a discrete lattice can take the values ± 1 at each site i of a lattice and $\langle \mathrm{ij} \rangle$ indicates summation over all pairs of nearest neighbor sites. The first term describes the ferromagnetic coupling (J>0) between the spins at sites *i* and *j*. This interaction is restricted to z nearest-neighbor pairs of spins. z is taken as 4 for this system. *H* is given by

$$\mathrm{H(t)=H_0 \cos(wt)}, \qquad + \tag{2}$$

where H_0 and w=2πν are the amplitude and the angular frequency of the oscillating field, respectively.

Since the dynamic method introduced and applied to study some dynamic behavior of a spin-1/2 Ising system under the influence of an oscillating magnetic field by Meijer and Edwards (Meijer and Edwards, 1969) in detail. We will give the derivation of the dynamic equations briefly. First, they focused attention upon the center spin of the cluster and a particular rim spin, say the *j*th. They denoted the probability that the center spin has a value σ_0 and the *j*th rim spin has a value σ_j by $P(\sigma_0, \sigma_j)$. Spin up (down), i.e., $\sigma = \pm 1$, means the magnetic moment and is parallel (antiparallel) to the magnetic field.

The master equation for the Probability vector **P** is found as

$$\frac{d}{dt}\mathbf{P} = \nu \begin{bmatrix} -3e^{\beta E_{++}} & e^{\beta E_{+-}} & e^{\beta E_{-+}} & e^{\beta E_{--}} \\ e^{\beta E_{++}} & -3e^{\beta E_{+-}} & e^{\beta E_{-+}} & e^{\beta E_{--}} \\ e^{\beta E_{++}} & e^{\beta E_{+-}} & -3e^{\beta E_{-+}} & e^{\beta E_{--}} \\ e^{\beta E_{++}} & e^{\beta E_{+-}} & e^{\beta E_{-+}} & -3e^{\beta E_{--}} \end{bmatrix} \mathbf{P} \tag{3}$$

where ν is a rate constant dependent upon the interaction of the spin system with the heat bath. Thus, the constant ν can be function of the temperature. The simplest assumption for this temperature dependence is to use an Arrhenius factor: $\nu_0 \exp(\frac{-U}{T})$ where U is an activation energy, which ensures that the rate will go to zero at T=0 as required.

Consider a pair of interacting spins with energy J that are acted upon by a time-dependent oscillating external magnetic field $H=H_0$Coswt. The energy of pair is

$$E = -\frac{J}{2}\sigma_1\sigma_2 - H(\sigma_1+\sigma_2) \tag{4}$$

The appropriate master equations is

$$\frac{d}{dt}\begin{bmatrix} P_{++} \\ P_{+-} \\ P_{-+} \\ P_{--} \end{bmatrix} = \nu \begin{bmatrix} -3e^{\beta E_{++}} & e^{\beta E_{+-}} & e^{\beta E_{-+}} & e^{\beta E_{--}} \\ e^{\beta E_{++}} & -3e^{\beta E_{+-}} & e^{\beta E_{-+}} & e^{\beta E_{--}} \\ e^{\beta E_{++}} & e^{\beta E_{+-}} & -3e^{\beta E_{-+}} & e^{\beta E_{--}} \\ e^{\beta E_{++}} & e^{\beta E_{+-}} & e^{\beta E_{-+}} & -3e^{\beta E_{--}} \end{bmatrix} \begin{bmatrix} P_{++} \\ P_{+-} \\ P_{-+} \\ P_{--} \end{bmatrix}, \tag{5}$$

where $E_{++} = -(\frac{J}{2}) - 2H$, $E_{--} = -(\frac{J}{2}) + 2H$, $E_{+-} = E_{-+} = (\frac{J}{2})$.

$<\dot{\sigma}_1>$, $<\dot{\sigma}_2>$ and $<\dot{\sigma_1\sigma_2}>$ can be found by using the definition of expectation value and the time dependent of the probability function, we obtain

$$<\dot{\sigma}_1> = -4\nu\sum \sigma_1 e^{\beta E} P(\sigma_1,\sigma_2) \tag{6-a}$$

$$<\dot{\sigma}_2> = -4\nu\sum \sigma_2 e^{\beta E} P(\sigma_1,\sigma_2) \tag{6-b}$$

$$<\dot{\sigma_1\sigma_2}> = -4\nu\sum \sigma_1\sigma_2 e^{\beta E} P(\sigma_1,\sigma_2) \tag{6-c}$$

where $e^{\beta E}$ is found using Eq.4,

$$e^{\beta E} = \exp\left[-\beta\frac{J}{2}\sigma_1\sigma_2\right].\left[-\beta H(\sigma_1+\sigma_2)\right] \tag{7}$$

Using some properties of the exponential function, the set of the dynamic equations are calculated as

$$\frac{d}{dt}<\sigma> = -4\nu e^{-\beta\frac{J}{2}} cosh(2\beta H)\left\{<\sigma> - \frac{1}{2}\tanh(2\beta H) - \frac{1}{2}\tanh(2\beta H)<\sigma_1\sigma_2>\right\} \tag{8}$$

$$\frac{d}{dt}<\sigma_1\sigma_2> = -2\nu e^{-\beta\frac{J}{2}}\left\{(e^{\beta J} + cos\,\mathrm{h}(2\beta H))<\sigma_1\sigma_2> -2sinh(2\beta H)<\sigma> - e^{\beta J} + cos\,\mathrm{h}(2\beta H)\right\} \tag{9}$$

We should notice that the quantity $<\sigma>$ replaces both $<\sigma_1>$ and $<\sigma_2>$ because of the homogeneity of the system. The system evolves according to the differential equation given by
Eq.(8) and Eq.(9) that can be written in the form,

$$w\frac{d}{d\xi}m = -4\nu e^{-\frac{J}{2T}} cosh[(2/T)(H_0 cos\xi)]\left\{<\sigma> - \frac{1}{2}\tanh[(2/T)(H_0 cos\xi)] - \frac{1}{2}\tanh[(2/T)(H_0 cos\xi)]<\sigma_1\sigma_2>\right\} \tag{10}$$

$$w\frac{d}{d\xi}q = -2\nu e^{-\frac{J}{2T}}\left\{(e^{\frac{J}{T}} + cos\mathrm{h}[(2/T)(H_0\cos\xi)]<\sigma_1\sigma_2> - 2\sinh[(2/T)(H_0\cos\xi)]<\sigma> - e^{\frac{J}{T}} + cos\mathrm{h}[(2/T)(H_0\cos\xi)]\right\} \tag{11}$$

where $m =<\sigma>,\ q =<\sigma_1\sigma_2>,\ \xi = wt,\ \beta = \frac{1}{kT}$ and $\nu = \nu_0\exp(\frac{-U}{T})$.

Solution and discussion of these equations are given in next section.

3. RESULTS AND DISCUSSION

In this section, we will find the dynamic phase transition (DPT) temperatures and present the dynamic phase diagrams. For these purposes, we first have to study the stationary solutions of the dynamic equations, given in Eqs. (10) and (11), when the parameters T, J and H0 are varied. The stationary solution of Eqs. (10) and (11) will be a periodic function of with period, that is and. Moreover, they can be one of two types according to whether they have or do not have the property

$$m(\xi + \pi) = -m(\xi) \tag{12}$$

A solution that satisfies Eq. (12) is called a symmetric solution which corresponds to a paramagnetic (P) solution. In this solution, the magnetization $m(\xi)$ oscillates around the zero value and is delayed with respect to the external field. Solutions of the second type, which do not satisfy Eq.(12), are called nonsymmetric; they correspond to a ferromagnetic (F) phase. In this case, the magnetization does not follow the external magnetic field anymore, but, instead of oscillating around a zero value, oscillates around a nonzero value. On the other hand, the correlation function $q(\xi)$ is oscillates around a nonzero value in both solutions. These facts are seen explicitly by solving Eqs. (10) and (11) numerically. Eqs. (10) and (11) are solved with the numerical method of the Adams-Moulton predictor corrector method for a given set of parameters and initial values and is shown in Fig.1. From the Fig.1, one can see those two different solutions, namely the paramagnetic (P) and the ferromagnetic (F) phases exist in the system. In Fig.1 (a), only the symmetric solution is always obtained, hence we have a paramagnetic (P) phase. On the other hand, in Fig.1 (b) only the nonsymmetric solution is always obtained; hence we have the ferromagnetic (F) phase.

Thus, Fig.1 displays that we have two solutions or phases in the system, namely paramagnetic (P) and ferromagnetic (F) phase or solutions. In order to see the dynamic boundaries between these two regions, we have to calculate dynamic phase transition (DPT) temperatures and then, we can present the dynamic phase diagram of the system. DPT temperatures are obtained by investigating the behavior the average magnetization in a period, also called the dynamic magnetization, as a function of the temperature. The average magnetization (M) and average correlation function (Q) in a period are given as

$$M = \frac{1}{2\pi}\int_0^{2\pi} m(\xi)\,d\xi \qquad \text{and} \qquad Q = \frac{1}{2\pi}\int_0^{2\pi} q(\xi)\,d\xi \tag{13}$$

The behavior of M and Q as a function of temperature for a value of J and H_0 are obtained by combining the numerical methods of Adams-Moulton predictor-corrector with the Romberg integration. We give one example to illustrate to characterize the nature (continuous and discontinuous) of transitions and to obtain the DPT temperatures, shown in Fig. 2. In Fig. 2, the thick line represents M and thin line represents Q. T_C is the second-order phase transition temperature. Fig.2 shows the behavior of M and Q as a function of the temperature for U=1, J=1 and H_0=0.1. In Fig.2 M decreases to zero continuously as the temperature increases, therefore the system exhibits a second-order phase transition. The second-order phase transition temperature, T_C is marked with a solid arrow in the figure,

T_C=0.1750. In this case the phase transition is from the F phase to the P phase. From Fig. 2, one can see that F phase region exists until T_C in the system and this fact is seen in the phase diagram of Fig.3, explicitly (compare in Fig. 2 with Fig.3.). On the other hand, average correlation function Q decreases to zero as the temperature increases and finally it becomes zero at infinite temperature as seen Fig.2.

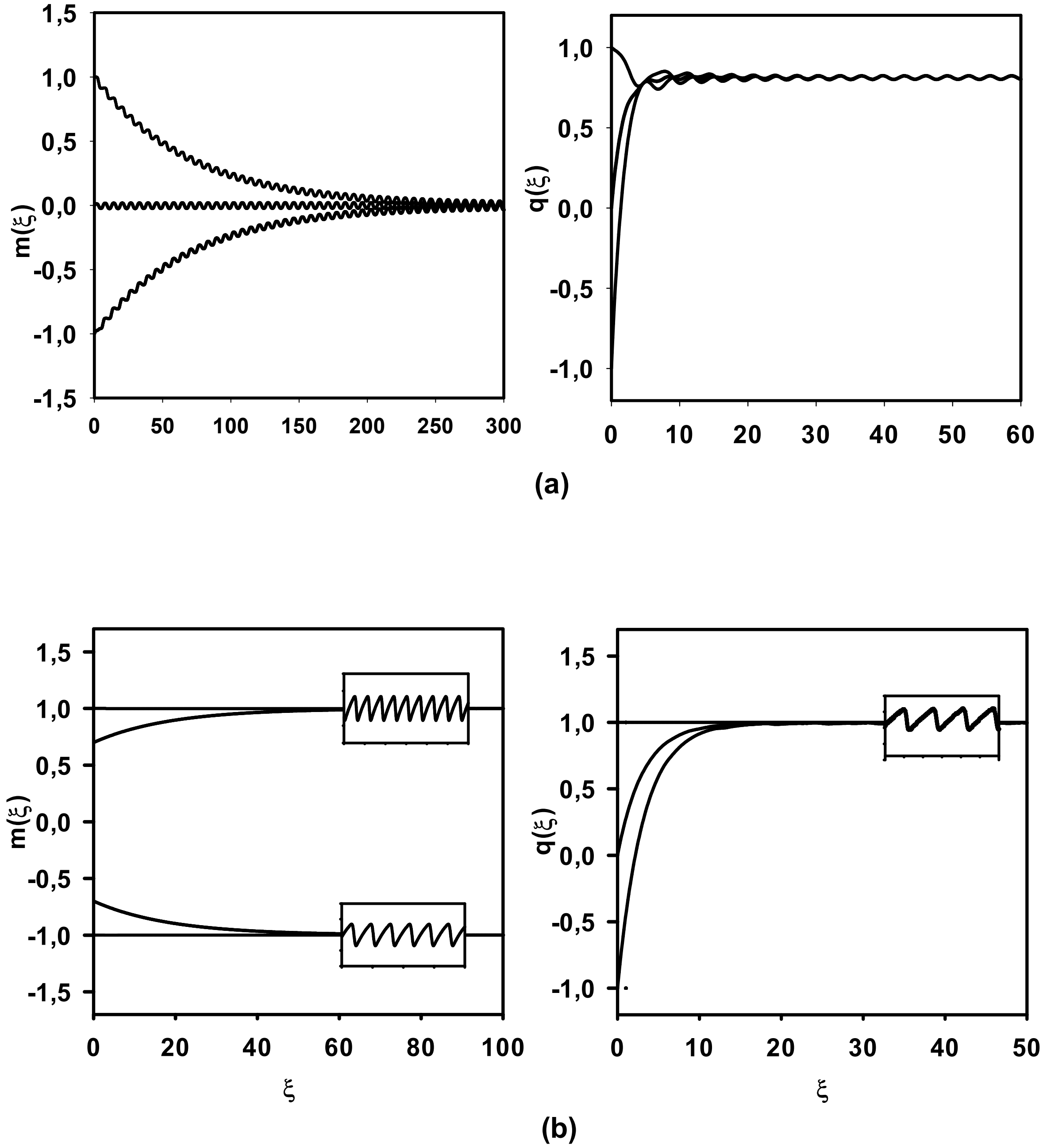

Figure 1. Time variations of the magnetization and correlation function ($m(\xi)$ and $q(\xi)$):

a) Only symmetric (paramagnetic) solution exists and is stable for U=1, J=1, H_0=0.6 and T=0.3.

b) Only nonsymmetric (ferromagnetic) solution exists and is stable for U=1, J=1,H_0=0.4 and T=0.1.

The dynamic phase diagrams of the system are calculated in the (T, H_0) plane and presented in Fig. 3 for several values of J. In these phase diagrams the solid line represents the second-order phase transition line. Fig. 3 represents the phase diagrams for U=1 and J=0.1, 1 and 2. In this phase diagram, the dynamic phase boundary is a second-order phase line which separates the F phase from the P phase. Moreover, one can see that F phase region becomes large for high values of J.

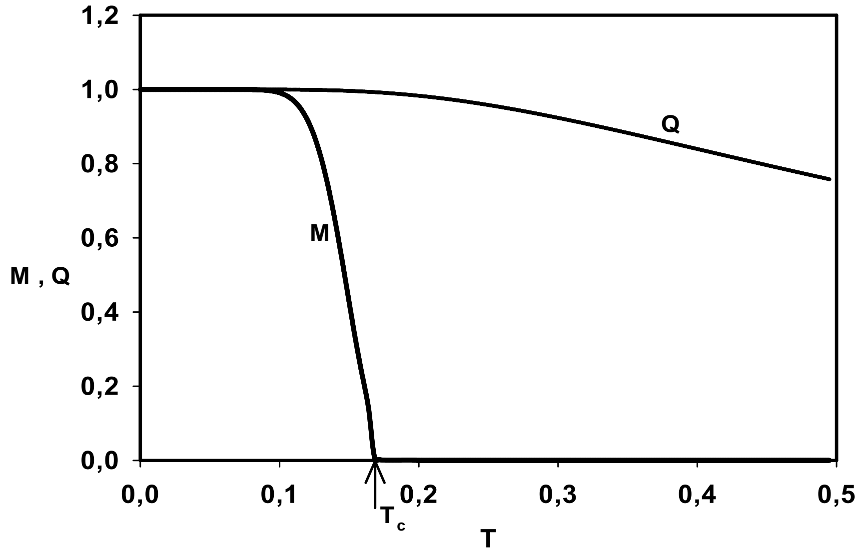

Figure 2. The average magnetization (M) and average correlation function (Q) are shown as a function of temperature for U=1, J=1 and H_0=0.1. Notice that, average magnetization (M) vanishes at T_C=0.1750.

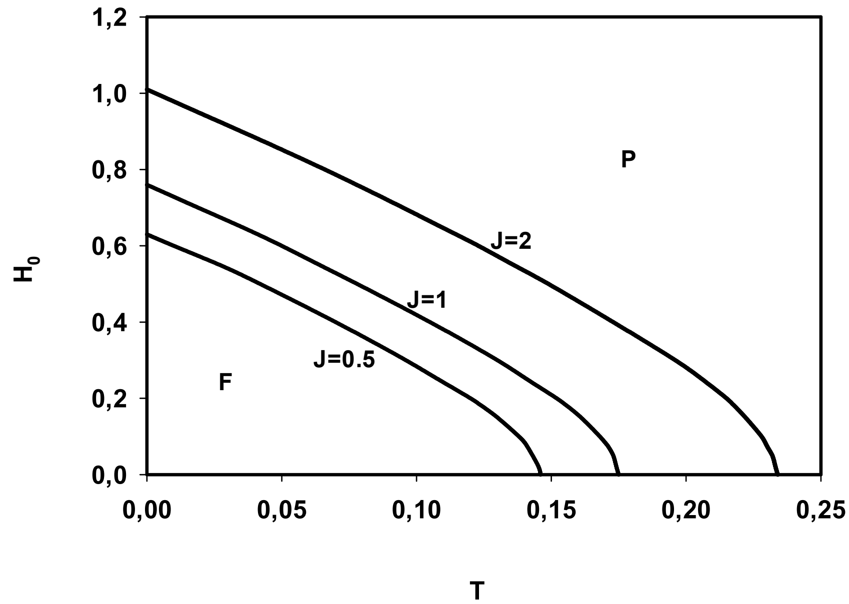

Figure 3. Phase diagram in the (T, H_0) plane for U=1 and J=0.5, 1 and 2. The paramagnetic (P) and ferromagnetic (F) phase regions are found. Solid lines represent the second-order phase transition temperature.

In conclusion, the dynamic phase transition (DPT) temperatures are always a second-order; hence there can be no tricritical point separating lines of first- and second-order dynamic phase transitions; therefore, this result is in good agreement with the dynamic MC simulations. Thus, we conclude or suggest that one can use this method for studying the DPT and presenting the dynamic phase diagrams in different systems instead of using the time consuming process searching dynamic critical behavior of systems while using the dynamic MC simulations.

REFERENCES

Acharyya, M. (1999). Nonequilibrium phase transition in the kinetic Ising model: Existence of a tricritical point and stochastic resonance, Phys. Rev. E, 59, 218. Doi: 10.1103/PhysRevE.59.218.

Acharyya, M., & Chakrabarti, B.K. (1995). Response of Ising systems to oscillating and pulsed fields: Hysteresis, ac, and pulse susceptibility, Phys. Rev. B, 52, 6550. Doi: 10.1103/PhysRevB.52.6550.

Chakrabarti, B.K., & Acharyya, M. (1999). Dynamic transitions and hysteresis, Rev. Mod. Phys., 71, 847. Doi: 10.1103/RevModPhys.71.847.

Fujiwara, N., Kobayashi, T., & Fujisaka, H. (2007). Dynamic phase transition in a rotating external field, Phys. Rev. E 75, 026202., Doi: 10.1103/PhysRevE.75.026202.

Gedik, N., Yang, D.S., Logvenov, G., Bozovic, I & Zewail, A.H. (2007). Nonequilibrium phase transitions in cuprates observed by ultrafast electron crystallography, Science, 316 (5823), 425-429. Doi: 10.1126/science.1138834.

Glauber, R.J. (1963). Time-dependent statistics of the Ising model, J. Math. Phys., 4, 294-307, Doi: 10.1063/1.1703954.

Jang, H., Azhari, M., & Yu, U. (2024). Monte Carlo study for the thermodynamic and dynamic phase transitions in the spin-S Ising model on Sierpiński carpet, Journal of Stat. Mech., vol. 2024, pp. 013201, January 2024, doi: 10.1088/1742-5468/ad0a91.

Jiang, F.L., Shi, X.L., & Liu, P.S. (2023). Dynamic magnetic properties and phase diagrams of Fe4N system, Int. J. Mod. Phys. B, 37 (17), 2350166., Doi: 10.1142/S0217979223501667.

Jiang, Q., Yang, H.N., & Wang, G.C. (1995). Scaling and dynamics of low- frequency hysteresis loops in ultrathin Co films on a Cu (001) surface, Phys. Rev. B 52, 14911., Doi: 10.1103/PhysRevB.52.14911.

Kantar, E. (2017). Dynamic magnetic behaviors in the Ising-type nanowire with core-shell single-ion anisotropies under a time-dependent oscillating external magnetic field, Chin. J. Phys., 55(5), 1808-1820., Doi: 10.1016/j.cjph.2017.06.013.

Kanuga, K., & Çakmak, M. (2007). Dynamic phase diagram derived from large deformation non-linear mechano-optical behavior of polyethylene naphthalate nanocomposites, Polymer, 48(24), 7176-7192., Doi: 10.1016/j.polymer.2007.09.047.

Kleemann, W., Braun, T., Dec, J., & Petracic, O. (2005). Dynamic phase transitions in ferroic systems with pinned domain walls, Phase Trans., 78(9), 811-816. Doi: 10.1080/01411590500289120.

Korniss, G., Rikvold, P.A., & Novotny, M.A. (2002). Absence of first-order transition and tricritical point in the dynamic phase diagram of a spatially extended bistable system in an oscillating field, Phys. Rev. E, 66, 056127. Doi: 10.1103/PhysRevE.66.056127.

Li, B., & Wang, W. (2024). Exploration of dynamic phase transition of 3D Ising model with a new long-range interaction by using the Monte Carlo method, Chin. J. Phys., 90, 15-30. Doi: 10.1016/j.cjph.2024.05.021.

Meijer, P.H.E., & Edwards, J.C. (1969). Dynamic behavior of a spin system with transverse coupling under the influence of an oscillating magnetic field, Annals of Physics, 54, 240. Doi: 10.1016/0003-4916(69)90152-3.

Samoilenko, Z.A., Okunev, V.D., Pushenko, E.I., Isaev, V.A., Gierlowski, P., Kolwas, K., & Lewandowski, S.J. (2003). Dynamic phase transition in amorphous YBaCuO films under Ar laser irradiation, Inorganic. Mat. 39-, 836-842., Doi:10.1023/A:1025025313382.

Temizer, Ü. & Demir, L. (2018). Dynamic magnetic features of the mixed Ising system on the bilayer square lattice, J. Supercond. Nov. Magn., 31, 889-903., Doi: 10.1007/s10948-017-4260-9.

Temizer, Ü. (2014) Dynamic magnetic properties of the mixed spin-1 and spin-3/2 Ising system on a two-layer square lattice, J. Magn. Magn. Mater. 372, 47-58., Doi: 10.1016/j.jmmm.2014.07.015.

Tome, T., & Oliveira, M.J. (1990). Dynamic phase transition in the kinetic ising model under a time-dependent oscillating field, Phys. Rev. A, 41, 4251. Doi: 10.1103/PhysRevA.41.4251.

Zimmer, F.M. (1993). Ising model in an oscillating magnetic field: Mean-field theory, Phys. Rev. E, 47, 3950, Doi: 10.1103/physreve.47.3950.